Environmental Measurements Methods

Automated stable isotope sampling of gaseous elemental mercury (ISO-GEM) – Insights into GEM emissions from building surfaces

Martin Jiskra, Nicolas Marusczak, Kin-Hung Leung, Lucas Hawkins, Eric M. Prestbo, and Jeroen E. Sonke

Environ. Sci. Technol., **Just Accepted Manuscript** • DOI: 10.1021/acs.est.8b06381 • Publication Date (Web): 22 Mar 2019

Automated stable isotope sampling of gaseous elemental mercury (ISO-GEM) – Insights into GEM emissions from building surfaces.

Martin Jiskra[1,2,*], Nicolas Marusczak[1], Kin-Hung Leung[3], Lucas Hawkins[4], Eric Prestbo[4], Jeroen E. Sonke[1,*]

[1]Observatoire Midi-Pyrénées, Laboratoire Géosciences Environnement Toulouse, CNRS/IRD/Université de Toulouse, 31400 Toulouse, France

[2]Environmental Geosciences, University of Basel, 4056 Basel, Switzerland

[3]Tekran Instruments Corp., M1P 2P4 Toronto, ON, Canada

[4]Tekran Instruments Corp., 98125 Seattle, WA, USA

*martin.jiskra@unibas.ch, jeroen.sonke@get.obs-mip.fr

Abstract

Atmospheric monitoring networks quantify gaseous elemental mercury (GEM) concentrations, but not isotopic composition. Here, we present a new method for automated and quantitative stable isotope sampling of GEM (ISO-GEM) at the outlet of a commercial Hg analyzer. A programmable multi-valve manifold selects Hg at the analyzer inlet and outlet based on specific criteria (location, time, GEM concentration, auxiliary threshold). Outlet Hg recovery was tested for gold traps, oxidizing acidic solution traps, and activated carbon traps. We illustrate the ISO-GEM method in an exploratory study on the effect of building walls on local GEM. We find that GEM concentrations directly at the building surface (wall inlet) are significantly enhanced (mean 3.8 ± 1.8 ng/m^3) compared to 3 m from the building wall (free inlet) (mean 1.5 ± 0.4 ng/m^3). GEM δ^{202}Hg (-1.26 ± 0.41 ‰, 1sd, n=16) and Δ^{199}Hg (-0.05 ± 0.10 ‰, 1sd, n=16) at the wall inlet were different from ambient GEM δ^{202}Hg (0.76 ± 0.09 ‰, 1sd, n=16) and Δ^{199}Hg (-0.21 ± 0.05 ‰, 1sd, n=16) at the free inlet. The isotopic fingerprint of GEM at the wall inlet suggests that GEM emission from the aluminum building surface affected local GEM concentration measurements. These results illustrate the versatility of the automated Hg isotope sampling.

Introduction

Mercury (Hg) is a global pollutant that is predominantly emitted to- and transported through the atmosphere as gaseous elemental mercury (Hg^0, GEM).[1, 2] Atmospheric dry deposition by vegetation uptake of GEM,[3] or wet deposition as Hg^{II} in rainfall and snowfall represent the dominant Hg source to aquatic and terrestrial ecosystems.[2] Local GEM concentrations are controlled by primary emission, deposition, in situ production from Hg(II) and re-emission processes.[3] Understanding the sources and processes that affect atmospheric GEM is essential to predict future ecosystem exposure to Hg. Current understanding of GEM dynamics and ecosystem loading is mainly based on concentration data from global Hg monitoring networks, but does not include source/process specific molecular or isotopic tracers.

Hg stable isotope measurements of GEM (which we use here interchangeably with TGM, total gaseous Hg) are a new tool to identify GEM emission sources and transformation processes and thus better understand atmospheric GEM dynamics.[4-9] Hg currently has 5 useful isotope signatures that represent mass dependent isotope fractionation (MDF: $\delta^{202}Hg$) and odd and even mass independent isotope fractionation (MIF: $\Delta^{199}Hg$, $\Delta^{200}Hg$, $\Delta^{201}Hg$, $\Delta^{204}Hg$). GEM sampled at terrestrial background sites far from anthropogenic emission sources is characterized by positive $\delta^{202}Hg$ values and slightly negative $\Delta^{199}Hg$ values.[5-7, 10, 11] Air affected by recent anthropogenic emissions exhibits mostly negative $\delta^{202}Hg$ values and $\Delta^{199}Hg$ values around zero, ranging from 0.2 to -0.2 ‰.[4, 5, 8, 9, 12] These values are similar to the Hg isotope composition of coal,[13-15] the dominant source of anthropogenic Hg emissions, illustrating the potential of Hg stable isotopes to fingerprint Hg sources.

GEM isotope signatures are very different from Hg^{II} in wet deposition, which has strongly positive $\Delta^{199}Hg$ and $\Delta^{200}Hg$.[7, 11] Studies show that vegetation and soil Hg have

Δ^{199}Hg and Δ^{200}Hg values that resemble more closely the isotope signatures of GEM than those of wet deposition.[7, 10, 11, 16, 17] Hg isotope mass balance of global soils and vegetation data suggest GEM plant uptake to be 3-4x larger than Hg wet deposition.[7] This has led to a re-appraisal of the foliar GEM uptake mechanism and the idea that the 'vegetation Hg pump' controls diurnal and seasonal GEM dynamics over terrestrial surfaces.[3]

Precise GEM isotope analysis, with 2σ uncertainty <0.1 ‰, requires 1000-fold more Hg (10 nanograms) than GEM concentration analysis (10 picograms). An additional challenge is that GEM isotope sampling recovery must be near-quantitative, to avoid isotope fractionation artifacts during sampling. Manual GEM isotope sampling methods thus far have used classical Hg sorbents, such as gold[4, 5, 11, 18] or various activated carbon powders,[6, 7, 10, 19, 20] and accumulated GEM over periods of 1 – 30 days. Such manual sampling complicates the study of short-lived (hours) pollution or chemical reactivity events, diurnal GEM dynamics, or spatial Hg isotope gradients. In addition, manual sampling only makes marginal use of atmospheric Hg monitoring network infrastructure.

The broader goal of this study was to design an automated stable isotope sampling application for GEM (ISO-GEM) able to resolve pollution or transformation events. The application should direct GEM isotopes onto multiple traps, based on predefined criteria, such as time (diurnal, other), space (multiple inlets), meteorology (temperature, humidity, wind direction) or pollution events (Hg or CO concentration triggers). The device ideally had to be compatible with the most common Hg analyzer used in Hg monitoring networks. More specifically, we focused on recovering analyzed Hg at the instrument detection cell outlet which has the advantage that Hg isotope recovery efficiency can be assessed from the GEM monitoring data. We tested different Hg trapping materials for GEM isotope sampling, and illustrate re-emission of GEM from building surfaces using the novel ISO-GEM sampling device.

Materials & Methods

Instrumentation

The Tekran® 2537X was developed in 2012 and expanded electronic command and control capabilities compared to earlier 2537 Models. The enhanced communication capabilities and modular firmware design provides the ability to develop research-specific tools such as the ISO-GEM application used in this research. The 2537X analyzer also provides remote controlled access to its operating software and firmware plug-in modules. The 2537X analyzer pumps ambient air at 1.5 L/min over a gold cartridge where the GEM is amalgamated and quantitatively trapped. During each 5 min collection cycle approx. 11 pg GEM are trapped on a gold cartridge if ambient air contains ~1.5 ng/m^3 GEM.[21] The trapped GEM is then thermo-desorbed and analyzed by atomic fluorescence spectroscopy (AFS) in high purity, dry argon (80 mL/min). After analysis the GEM is exhausted by the cell vent at the back of the 2537X, where it is re-captured for Hg stable isotope analysis. A dual pair of gold cartridges allows continuous measurement, one cartridge collects GEM while the second one is analyzed. With the added capabilities of the 2537X, Tekran designed and manufactured a programmable multi-port sampling system (Tekran® 1115i) specifically adapted for automated GEM isotope sampling (ISO-GEM). The firmware plug-in controls the function of the Tekran® 1115i multi-valve manifold, determining both how the 2537X analyzer collects sample and the post-analysis flow path of the mercury measured by the instrument. The 1115i plug-in controls all valve positions, which are synchronized with the 2537X 5-min analysis cycles. The 1115i multi-valve manifold was outfitted with 3 large 3-way valves (NResearch 648T032 with PFA 1/4'' connectors), and 5 small 3-way valves (NResearch 225T032 with PFA 1/8'' connectors). The 3 large valves permit regular flow rate (1.5 L min^{-1}) sampling of GEM at

up to 4 different physical locations (e.g. gradient, inside vs. outside a building, etc.). The 5 smaller valves are used to direct exhausted Hg at the 2537X cell vent, in a high-purity, dry argon flow rate of 80 mL min^{-1}, to the dedicated Hg isotope traps. Inlet lines to the 2532X Tekran consisted of 1/4'' PFA tube and exhaust lines consisted of 1/8'' PFA tube. The original brass cell vent of the Tekran® 2537X was replaced by a PTFE cell vent to prevent potential sorption of GEM.

Atmospheric Temperatures were obtained for Toulouse-Blagnac (43.62°N, 1.39°E) close to the GET Laboratory building through the French Meteo services (www.infoclimat.fr).

Hg trapping methods

Two trapping methods have been previously used to collect nanogram quantities of GEM for isotopic analysis: (i) amalgamation of GEM on gold coated quartz beads,[4, 5, 11, 18] and (ii) activated carbon traps impregnated with halogens (Cl, I)[6, 7, 10, 19, 20] or sulfur.[22, 23] A third method that is commonly used to trap GEM, not during ambient GEM sampling, but as part of laboratory pre-concentration methods, consists of purging GEM through a strongly oxidizing, acidic aqueous solution.[13, 24] There are important differences between direct manual sampling of GEM onto gold or activated carbon, and the ISO-GEM application: 1. Direct sampling is done in air at 1-2 L min^{-1} flow rates, while 2537X cell vent trapping is done in low flow (80 mL/min) high purity, dry argon. 2. Direct sampling onto multiple, parallel gold traps is done for at most 1-3 days, while 2537X cell vent trapping in ISO-GEM applications will typically last 1-6 weeks in line with routine instrument maintenance schedules. The ISO-GEM trapping method therefore has to be robust and free of Hg breakthrough over prolonged sampling times. We tested several GEM trapping methods, namely gold-quartz traps, acid-traps and activated carbon traps impregnated with iodine (I-AC) and sulfur (HGR-AC). As the goal of this project was to

develop an optimal ISO-GEM system, we chose an iterative development scheme, which may result in the fact that not all conditions have been tested for all trapping materials.

Gold coated quartz bead traps (Ref. # *35-26510-00*), and solid gold matrix traps (Ref. # 35-25500-00) were obtained from Tekran® Instruments. Iodated activated carbon powder (I-AC) was obtained from Brooks Rand. Sulfur impregnated activated carbon (Calgon HGR-AC, product no 2300, Calgon Carbon Corp.) was provided by F. Wania at the University of Toronto at Scarborough. I-AC (125mg) and HGR-AC (400 mg) powder was weighed and traps were prepared manually in 12cm long Pyrex tubes (7 mm OD, 4 mm ID); the powder was held in place by a diameter constriction of the tube and two quartz wool plugs. Halogen sorbent traps, used to eliminate volatile iodine, were obtained in the form of LECO AMA-254 catalyst tubes (part No. 614-822-105) from Symalab (France) and manually prolonged by 20 cm. Bi-distilled HNO_3 and HCl was produced in-house, and high purity oxygen and ultra high purity dry (UHP) argon gas was obtained from Air Products, France.

Hg concentration analysis

All analyses were performed at the temperature controlled (21±1°C) Geoscience Environnement Toulouse laboratory. Both gold bead and gold matrix traps were desorbed and analyzed by dual amalgamation atomic fluorescence spectrometry (AFS, Brooks Rand Model III, USA). The AFS was calibrated using manual GEM vapor injections from an in-house thermostatted liquid/vapor Hg source.

I-AC and HGR-AC traps were processed using protocols adapted from Fu et al. 2014.[19] The method is based on dual-tube furnace combustion in an AMA-254 halogen trap. I-AC and HGR-AC was combusted in a first oven under a continuous flow of Hg-free O_2 (75 mL/min) over 6h by ramping temperature to 680°C (ramp 1: 5°C/min to 120°C,

ramp 2: 1°C/min to 250°C, ramp 3: 2°C to 680°C). The I-AC and HGR-AC powders were placed in 10 cm quartz tubes closed with quartz wool. To increase the life-time of the catalyst tube and to reduce wall sorption of GEM the activated carbon traps were embedded with 1g of additional trapping material on each side (Figure S1). For I-AC a halogen scrubber (mixture of MnO_2 (70% w/w), CoO (20 % w/w) and CaO (10%w/w, pre-baked at 680°C for 2h) was used following the SDS 06112 of the AMA-245 (Leco) and for HGR-AC sodium bicarbonate (Na_2CO_3, pre-baked at 500°C for 2h) was used following McLagan et at. 2017.[25] The second oven housed the halogen scrubber section, which was constantly kept at 680°C. After the combustion oven GEM was introduced into a 8 mL oxidizing solution trap consisting of 40 volume% inverse aqua regia (iAR, 4.2 N HNO_3, 1.2 N HCl) in a 15mL Falcon tube. A custom-made type#3 (16-40 µm) porosity glass bubbler tube was used to generate small diameter bubbles.

Total Hg concentrations in 40vol%iAR solutions were measured after dilution following the USEPA 1631 method.[26] Aliquots of 0.2 - 2 mL were analyzed in duplicate on a semi-automatic cold vapor atomic fluorescence spectrometry (CV-AFS, Brooks Rand Model III, USA) using a single gold trap.

Hg levels recovered from different traps and measured by AFS were compared to GEM measurements of a Tekran® 2537X analyzer to determine sampling yields. The analyzer was regularly (23h) calibrated using its internal GEM permeation source, and was monthly calibrated by manual GEM vapor injections from the external GEM vapor source. All manual calibrations agreed within 5% of the permeation source calibration over the 2 years of research.

Blank levels of the I-AC and HGR-AC powders were measured using a DMA-80 (Milestone) mercury analyzer.

Table 1: Summary of the performance of different tested trapping materials for Hg stable isotope sampling. *Samples collected at the exit of the Tekran 2537X cell vent in an ultra high purity, dry (UHP) argon matrix. This does not represent trapping efficiency in ambient air. BDL stands for below detection limit, numbers in brackets represent range. **including data reported in Ref.[10]

Trap material	**gold-trap***	**acid-trap***	**I-AC**	**HGR-AC**
description	gold surface or sand beads coated with gold	40% inverse Aqua regia	Iodine impregnated (10% w/w) activated carbon	Sulfur impregnated activated carbon
Matrix	UHP Argon	UHP Argon	ambient air	ambient air
trap flow (mL/min)	80	80	~300	~300
Time sampled	1-70 h	24-210 h	48 – 62 d	48 – 62 d
Hg amount (ng)	0.2 – 12	6-13	11-32	21-39
Recovery (%)	66% ± 27% (n=15)	94% ± 9% (n=13)	97 ± 39 % (n=10)**	95% ± 4% (n=4)
Breakthrough	11% (2-19, n=12)	<2 % (n=1)	BDL	BDL
Blank (ng/trap)	BDL	0.1 ± 0.04	0.32 ± 0.1	0.06 ± 0.03
advantage	Simple handling and good recovery for short sampling periods (<16h)	Direct analysis of the trap by MC-ICPMS	Good performance	Very good performance
disadvantage	Passivation of gold traps at sampling times exceeding	i) Handling acids requires training	i) Additional oven	(i) Additional oven

	16h (at 1.5 L/min sampling rate)	and safety measures. ii) Acid trap might lead to an increase in pressure in the Tekran measurement cell iii) Needs cooling for longer trapping periods	combustion step (ii) Matrix effects possible on the MC-ICPMS if the halogen scrubber did not work efficiently	combustion step

186

187

188 **Hg stable isotope analysis**

189 Hg isotope ratios were analyzed by cold vapor multi-collector inductively coupled plasma
190 mass spectrometry (MC-ICP-MS, Thermo-Finnigan Neptune) following published
191 protocols.[24] Hg isotope composition is reported in delta notation (δ) in per mil (‰) by
192 referencing to the bracketed NIST 3133 Hg standard:

193 $\delta^{xxx}Hg=(^{xxx/198}Hg_{sample}/\,^{xxx/198}Hg_{NIST3133}-1)\times10^{3}$ (1)

194 where 'xxx' refers to measured isotope masses: 199, 200, 201, 202 and 204. MIF is
195 reported in capital delta (Δ) notation (‰), which is defined as the difference between the
196 measured $\delta^{199}Hg$, $\delta^{200}Hg$, $\delta^{201}Hg$ and $\delta^{204}Hg$ and those predicted from $\delta^{202}Hg$ using the
197 kinetic MDF law:

198 $\Delta^{xxx}Hg=\delta^{xxx}Hg-\beta_{xxx}\times\delta^{202}Hg$ (2)

199 where the mass-dependent scaling factor β_{xxx} is 0.252 for ^{199}Hg, 0.502 for ^{200}Hg, 0.752 for
200 ^{201}Hg and 1.493 for ^{204}Hg. The long-term uncertainty was evaluated by repeated
201 measurement of the ETH-Fluka Hg standard, which yielded values of -1.45±0.19‰,
202 0.08±0.09‰, 0.02±0.09‰, 0.03±0.09‰, -0.03±0.2‰ (2σ, n=10) for $\delta^{202}Hg$, $\Delta^{199}Hg$,

Δ^{200}Hg, Δ^{201}Hg and Δ^{204}Hg, respectively, in agreement with the published values [17, 27]. The 2σ uncertainties of isotope compositions for ETH-Fluka were taken as the typical analytic uncertainties of isotope compositions for samples. If the 2σ uncertainties of isotope compositions for samples with multiple measurements were larger than the typical 2σ uncertainties, then the 2σ uncertainties of samples applied.

Results & Discussion

Cell vent trapping efficiency on gold in argon

Initially gold bead traps were directly connected to the 2537X cell vent using 1/8'' FEP tubing, and without presence of the 1115i valve module. GEM from the cell vent was loaded onto the traps for time periods ranging from 1 to 70 hours. Two traps were placed in series to monitor potential Hg breakthrough. Trapping recoveries were measured by manual gold trap desorption with AFS detection and were variable, from 10-88%, with 4 out of 6 recoveries considered as low, <85% (Figure 1, Table S1). The 85% cut-off is defined by the combined analysis uncertainty of sampled Hg by the Tekran® 2537X (15%, 2σ), and of recovered Hg by AFS (15%, 2σ). All secondary, in-series, gold traps showed signs of breakthrough and did not recover all GEM vapor lost by the first trap, suggesting that the secondary traps too suffered from Hg breakthrough (Table S1).

Next, we investigated gold matrix trap performance by loading 1-70 hours of cell vent GEM in argon onto the traps during regular 2537X operation (Figure 1). During 4 out of 9 tests, in series gold matrix traps were used to assess breakthrough. Recoveries were found to range from 38-98%, with 3 out of 5 long loading experiments having recoveries <80%. Again, in-series traps in 2nd position showed significant Hg breakthrough in the argon matrix (Table S1).

Finally, gold matrix traps were loaded with controlled amounts of GEM vapor from the 2537X internal permeation source, also in high purity argon matrix. During 4, 7, 13 and 16 hours, 1-4 ng of permeation source GEM vapor was loaded onto the gold traps. Recoveries measured by manual trap desorption with AFS were 86-99% (Figure 1), which is within the combined analysis uncertainty of the methods.

In summary, we observed that gold traps placed at the 2537X cell vent showed good recovery, >80%, of loaded GEM over time periods <16 hours. For atmospheric GEM loading times from 17-70 hours recoveries were incomplete. Overall the performance of gold traps over longer time periods at the cell vent was unexpected and likely related to the gradual passivation of the gold surface. After heating the gold traps for analysis, they performed normally, indicating no degradation of the trap. Adding a soda-lime trap prior to the gold trap has been shown to increase the performance of gold traps.[19] We stress that our findings by no means question the use of gold traps in standard GEM vapor analyzers sampling ambient air, including the Tekran® 2537X used here, with very short Hg loading times generally ranging from 2 to 10 minutes.

Cell vent trapping efficiency in oxidizing solution in argon

We evaluated the acid traps consisting of 40vol% iAR oxidizing solution traps by directing variable amounts (6-14 ng) of ambient GEM or 2537X permeation source GEM to the traps, without presence of the 1115i valve manifold (Table S2). Solution Hg concentrations were analyzed by CV-AFS and recoveries found to be good, in the range of 85-104%. We subsequently connected the 1115i valve module, with its multiple tees and connectors. Thirteen ambient GEM tests, loading 4-18 ng of Hg over 22-70 hours, were performed with good recoveries ranging from 85-111 % (Figure 1).

We observe a 6-22 % volumetric loss of the 40 % iAR solutions after 25-70 hours of Hg trapping at ambient laboratory temperature for the first four samples, 1-4. This volumetric loss did not an effect on the Hg trapping efficiency, as recoveries were 89-110 % for samples 1-4. Indicating soda lime traps at the solution trap outlet did not show any color change suggesting that the weight loss is mostly water, rather than acid. Nevertheless, a loss of 22 % over 3 days can potentially become problematic for longer sampling periods (7-14 day). To reduce the volume loss, we tested trapping with a manual cooling system that maintained a temperature of 5-6°C. The solution traps were placed inside a polystyrene cooler, filled with ice-packs that were changed every 2 days. This system effectively reduces the volume loss by evaporation to <6%.

Carry-over of GEM from the permeation source calibration cycles to sample traps was tested. We connected the sample inlet of the Tekran® 2537X to a zero-air cartridge and collected cell-vent GEM for 48-72h, after routing calibration pulses of the permeation source (once every 2h) to a separate trap. We found that less than 2% (n=2) of perm-cell Hg was transferred to subsequent samples and conclude that carry-over from the permeation source to the following sample did not cause any significant bias in ISO-GEM measurements.

We tested the Hg from the permeation cell calibration unit as internal standard for Hg stable isotope measurements by trapping the calibration cycle GEM pulse on a dedicated valve position and found very consistent δ^{202}Hg and Δ^{199}Hg values, over multiple (n=5) test days (Figure 2). Please note that we tested only one instrument and that the uniformity of the permeation source Hg isotope composition from other instruments has to be confirmed.

In summary, acid traps based on 40%-iAR provide a good cell vent trapping with high recovery, low break-through and low blanks. A major advantage is the direct

measurement of the (2x diluted) acid on the MC-ICPMS without further pre-enrichment steps. Acid traps however have the drawback of acid being handled in the field and during shipment which can cause higher costs/efforts for logistics and personal safety.

trapping efficiency on activated carbon in ambient air

We evaluated the efficiency of iodine activated carbon (I-AC) and sulfur-impregnated activated carbon (HGR-AC) traps by pumping ambient air over the traps for prolonged periods (48 – 62 days) at a flow rate of 0.3 L/min. We expect a similar performance of I-AC and HGR-AC traps in 80 mL/min Argon at the cell vent of the Tekran® 2532X analyzer compared to the 4 times higher flowrate of ambient air tested here.

Breakthrough of I-AC and HGR-AC traps was measured after two months of continuous sampling of at 0.3 L/min, by connecting the traps to a Tekran® 2537X analyzer and pumping ambient air over the traps at 1 L/min. For both carbon traps, I-AC and HGR-AC the Hg concentration measured after the trap was below the detection limit (<0.1 ng/m^3), indicating that there was no measurable breakthrough.

Both, I-AC and HGR-AC showed good recoveries, however the reproducibility for HGR-AC (94 ± 4 %, n=4) was better than for I-AC (97 % ± 39 %, n=10)(including data from Ref.[10]). The blank for I-AC was 2.6 ± 0.8 ng/g and for HGR-AC was 0.16 ± 0.06 ng/g. Considering the different amounts of powder used for the traps, this resulted in absolute Hg amounts of 0.32 ng and 0.06 ng per trap for I-AC and HGR-AC, respectively.

Based on our experience, IC powder is more challenging to combust as it liberates large amounts of volatile iodine compounds that need to be removed from the combustion carrier gas using halogen traps. If not, the iodine will form strong Hg-iodide complexes in the oxidizing solution trap, which may affect Hg isotope analyses by an incomplete reduction of Hg(II)-iodide during cold-vapor generation. Sulfur generates gaseous SO_2,

which partly becomes sulfuric acid in the oxidizing solution trap and does not interfere later on with Hg(II) reduction by Sn(II).

In summary, we found both 40vol%iAR oxidizing solution traps and activated carbon based I-AC and HGR-AC traps to recover GEM quantitatively at the 2537X cell vent over prolonged periods of sampling. The three types of traps have different advantages and disadvantages (Table 1). Solution traps require no further processing, other than dilution to 20vol%iAR, before direct Hg isotope measurement. The solution traps need to be cooled however, to avoid evaporation of the acidic solution, and shipping acidic solutions from sampling site to laboratory requires strict safety precautions. Handling and shipping of I-AC and HGR-AC traps is more convenient, however they require further processing by dual tube furnace combustion methods to recover trapped Hg for isotopic analysis. The choice of trap type has to be made on an individual basis depending on the research question and logistical settings (e.g. long-term vs. short-term campaign).

ISO-GEM multi-valve manifold configuration

The Tekran® 1115i multi-valve manifold we tested is equipped with 5 small valves and 3 large valves (Figure S2). The small valves can be connected in a parallel or tree configuration to the 2537X cell vent (Figure S3) and guide GEM vapor to 4 or 5 different GEM isotope traps. The three large valves can be configured either at the 2537X inlet to sample different physical sources of Hg (outside/inside; night/day; etc.) or be used at the cell vent for additional GEM trapping capacity.

One GEM isotope trap is exclusively dedicated for the mercury coming from the permeation source in the aim to not have a contribution to ambient air samples and bias in the Hg isotopic ratios. Permeation source GEM also serves as internal Hg isotope standard.

The 1115i multi-valve manifold is directly programmed by the intuitive plugin developed by Tekran® (Figure S4). This plugin allows to program the 1115i according to different criteria chosen by the user. For each event (e.g. inside building during nighttime) a series of valve positions (open vs. closed) are defined, determining which air mass is analyzed (e.g. inside vs. outside) and directing the GEM to a designated isotope trap after analysis (Figure 3A and Figure S5 – S7). This allows for the automated sampling of air collected under pre-defined conditions (e.g. time, location, Hg amount). The plugin monitors the status and timing in the programming and actuates the solenoid valves according to the program synchronized with the measurement cycle of the 2537X. The user will also assign any programmed event-flags in the sample data recorded by the 2537X. These flags provide positive indication of 1115i operations performed during each sampling period and allow to calculate trapping yields on individual traps.

The following events can be programmed by the Tekran® 1115i plugin.

(i) **A/B- cycling.** This event switches the valve position every A/B cycle (usually 10 min) between customized valve positions, to e.g. quasi-simultaneously measuring and sampling at different locations (e.g. gradient, inside/outside, etc.) (Figure S5).

(ii) **time event.** For this event, a start time and an end time must be defined in the 1115i plugin. In this example, we program a nighttime period and a daytime period on separate ports (valves) (Figure S6).

(iii) **GEM threshold event.** This event will be a function of the Hg concentration measured by the 2537X. In the plugin we specify a threshold of GEM concentration allowing to switch a valve and load GEM to a different trap. Any GEM concentration higher than the specified value will trigger a set of valve state and flag (Figure 3A).

(iv) **ADC trigger input event.** The ISO-GEM application can be configured with an external trigger from an auxiliary sensor (e.g. O_3 or CO analyzers) or program. An analog signal (up to 5V) can be sent by an external source to the 1115i plugin and the valve positions are switched when a certain pre-defined threshold is reached. Note that we did not have time to test this feature. (Figure S7)

ISO-GEM application to building emissions

In an exploratory study we used ISO-GEM to investigate the GEM emission from a building surface and its effect on spatial GEM concentrations. In different settings we programmed ISO-GEM to quasi-simultaneously measure inside and outside the building (i – A/B cycling), to distinguish between day and night (ii – time event) and to distinguish between GEM concentration levels (arbitrary GEM threshold: >3 ng/m^3 and <3 ng/m^3, iii – Hg amount event) (Results in Table S3). Furthermore, we sampled GEM at two different locations outside the GET laboratory building, close to the building surface (wall-inlet, 1.2 m above ground) and 3m away from the building (free-inlet, 2m above ground) (Figure 4A). The building wall consists of powder coated aluminum siding.

The air sampled at the wall inlet was characterized by relatively high GEM concentrations (3.8 ± 1.8 ng/m^3, mean and 1σ on 1h means) and Hg stable isotope signatures showed negative δ^{202}Hg values (-1.26 ± 0.41 ‰, 1sd, n=16) and circum-zero Δ^{199}Hg values (-0.05 ± 0.10 ‰, 1sd, n=16). GEM concentrations measured at the free inlet of 1.5 ± 0.4 ng/m^3 (mean and 1σ on 1h means) were similar to Northern Hemispheric background levels of ~1.5 ng/m^3.[21] Hg stable isotope signatures measured at the free inlet (δ^{202}Hg = 0.77 ‰ ± 0.08 ‰, Δ^{199}Hg = -0.22 ‰ ± 0.04 ‰ , mean and 1σ, n= 7) agreed well with measurements reported for background sites in France and the US (δ^{202}Hg = 0.53 ‰ ± 0.37 ‰, Δ^{199}Hg = -0.22 ‰ ± 0.05 ‰ , mean and 1σ, n= 59)(Figure 2).[5-7, 10] The

similar Hg isotope signatures and Hg concentrations measured at the free inlet in suburban Toulouse compared to Northern Hemispheric background sites suggests that GEM was dominated by long-range transport background GEM and that the contribution from local anthropogenic sources and local building emission was minor.

Using the time event (ii) function, we collected the air at the wall inlet sampled during daytime and nighttime on two different traps. Daytime air was characterized by higher GEM concentrations (3.5 ± 0.8 ng/m^3, n=3) than nighttime air (2.6 ± 0.3 ng/m^3, n=3). The higher GEM concentration of daytime air was concomitant with more negative δ^{202}Hg values (-1.82 ‰ ± 0.37 ‰, n=3) than nighttime air (-1.36 ‰ ± 0.17 ‰, n=3). Δ^{199}Hg values were similar between daytime (-0.03 ‰ ± 0.09 ‰, n=3) and nighttime air (-0.03 ‰ ± 0.11 ‰, n=3). The higher GEM concentrations during daytime observed at the wall inlet is opposite to observations from other urban sites, where highest GEM concentrations were observed in the early morning when the nocturnal boundary layer was most stable.[28, 29] This suggests that the high GEM concentrations measured at the wall inlet were affected by local emissions from photo-chemical or temperature related processes (see discussion below).

Using the GEM threshold event (iii) function we separated the outside air of the wall inlet on two different traps using a threshold of 3 ng/m^3 (Figure 3). δ^{202}Hg was more negative for the trap with higher concentration (>3 ng/m^3, mean GEM = 3.9 ng/m^3, δ^{202}Hg = -1.54 ‰) compared to the trap that collected lower GEM (<3 ng/m^3, mean GEM = 2.8 ng/m^3, δ^{202}Hg = -1.19 ‰).

Combining all wall and free outside measurements, we found a strong linear correlation between the δ^{202}Hg signature and the Hg concentration of GEM expressed as 1/Hg (R^2 = 0.91, p<0.001, Figure 5C) as well as between Δ^{199}Hg and 1/Hg (R^2 = 0.57, p<0.001, Figure 5D). This strong correlation suggests that outdoors GEM can be explained

by two distinct sources, GEM emission from the local building and GEM from background air. The high variability of the GEM concentration at the wall-inlet (Figure 4 B) and the extent of mixing between GEM emission from the building with GEM from background air is likely controlled by the turbulence of air in proximity to the building.

Mercury concentrations in buildings can be highly elevated compared to outdoor ambient air concentrations.[30] It has been suggested that 10% of the households in the United States exhibit indoor GEM concentrations exceeding the U.S. reference concentration of 300 ng m^{-3}.[30] Hg has been used as biocide in paint in between 1950 and 1990 and was thus intentionally employed in buildings.[31] A second source of Hg in buildings are micro-spills through the accidental release from products containing Hg, such as e.g. thermometers or fluorescent light-bulbs.[30] Using the A/B-cycle (i) sampling scheme we measured the GEM concentration quasi-simultaneously inside and outside the GET laboratory building in Toulouse. The GEM concentration inside the building was 3.61 ng/m^3, whereas the outside concentration was 2.45 ng/m^3 during the same period. Given that the concentration difference was relatively small (1.2 ng/m^3) and all the windows of the building were permanently closed, we assume that emission from inside the building contributed insignificantly to the elevated GEM concentrations measured at the wall inlet.

Elevated GEM concentrations outside buildings have been reported for several urban areas with e.g. 2.7 to 3.8 ng/m^3 in New York,[32] 2.0 ng/m^3 in Windsor, ON close to Detroit,[33] 1.9 ng/ m^3 in Toronto[34] and 9.7 ng/m^3 in Guiyang, China.[35] Carpi and Chen suggested that elevated GEM concentrations in urban areas were related to re-emission of GEM from building and other urban surfaces.[32] They suggest that the GEM originates from photochemical reduction of divalent Hg that has previously been deposited through dry deposition.[32] Preliminary measurements of divalent Hg in precipitation at the Toulouse site (data not reported here in detail; Δ^{200}Hg = 0.12 ‰ ± 0.11 ‰, n=4) are in

agreement with precipitation data measured elsewhere.[4, 7, 11, 36, 37] The Δ^{200}Hg values of GEM samples at the wall inlet (-0.04 ‰ ± 0.06 ‰, n=16) was very similar to that of GEM measured at the free inlet (-0.06 ‰ ± 0.04 ‰, n=7) or at remote sites (-0.04 ‰ ± 0.03 ‰, n=39). [5,6, 7,5, 10] Aluminum, the material of the building facade, can form an amalgam with Hg.[38] Hg in the building wall may originate from dry deposition of GEM from the atmosphere during colder winter months (i.e. through amalgamation by the aluminum building material) rather than from dry deposition of divalent Hg which would be expected to exhibit positive Δ^{200}Hg anomalies. With the data presented here we cannot exclude the presence of residual Hg from the production process of the building material and a contribution to the re-emission observed. There are no experimental studies investigating Hg stable isotope fractionation during volatilization of GEM from aluminum amalgam, however the isotopic signatures at the wall inlet agree with the volatilization of GEM from liquid Hg, with negative δ^{202}Hg and small positive Δ^{199}Hg in the vapor phase.[39, 40] GEM concentrations at the wall inlet were positively correlated with the ambient air temperature (R^2 = 0.21, $p<0.001$, Figure S8) in agreement with previous findings,[32] suggesting that the re-emission flux was favored by higher temperature or solar irradiation.

The exploratory results of the ISO-GEM application illustrate the potential of smart automated sampling strategies based on pre-defined criteria (e.g. time, location, internal (GEM concentration) and triggers from external sensors (O^3, wind direction)) to maximize the information of the Hg stable Hg isotope finger printing tool. At the same time the elevated GEM concentration and distinct Hg stable isotope signatures measured at the wall inlet close to the building surface illustrate how air can be affected very locally by building emissions. This has important implications for atmospheric GEM monitoring

stations, where sample inlets have to be placed carefully in order to avoid measurement bias from local building emission.[41,42]

Financial Interests:

The automated multi-valve module (1115i) at the center of the ISO-GEM application is commercially available from the Tekran® Instruments Corporation. We would like to mention that the conceptual ISO-GEM idea can be implemented by a custom-made instrumentation and control software without purchase of the 1115i module.

Acknowledgments:

This work was supported by ERC-2015-PoC_665482 grant from the European Research Council to JES, and by the Tekran® Instruments Corp. MJ received funding through the H2020 Marie Sklodowska-Curie grant agreement 657195 and Swiss National Science Foundation grant PZ00P2_174101.

Supporting Information:

Additional figures, and tables. The Supporting Information is available free of charge on the ACS Publications website at DOI:

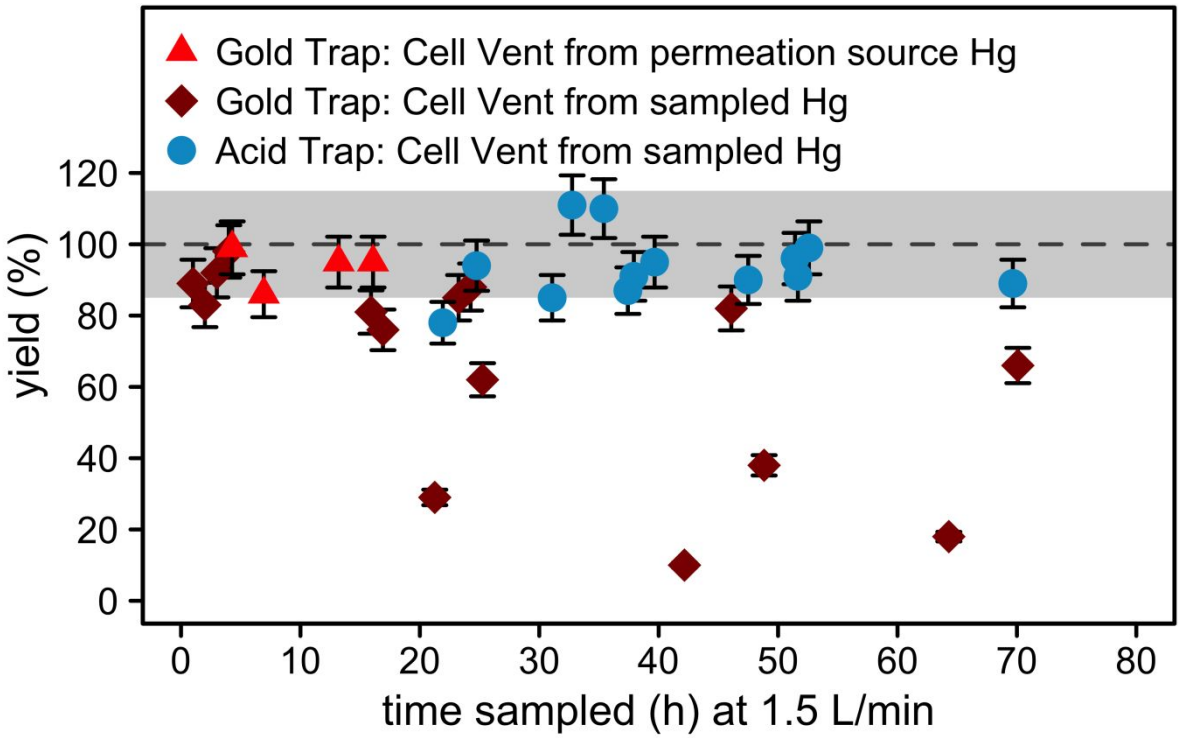

474

475

476 **Figure 1:** Sampling yields (%) of GEM recovered in high purity argon by different trap
477 methods at the outlet of a Tekran® 2537X analyzer relative to Tekran® GEM concentration
478 measurements. GEM from ambient air was recovered at the cell vent by gold-traps (red
479 diamonds) and acid-traps (blue circles). GEM from the permeation source recovered from
480 the cell vent in argon with gold-traps is shown as red triangles. The error bars represent
481 7.5% (1σ) uncertainty of combined AFS measurements. The dashed line represents 100
482 % sampling yield and the shaded area represent the interval of 85% - 115% yield that is
483 expected acceptable for Hg stable isotope measurements.

484

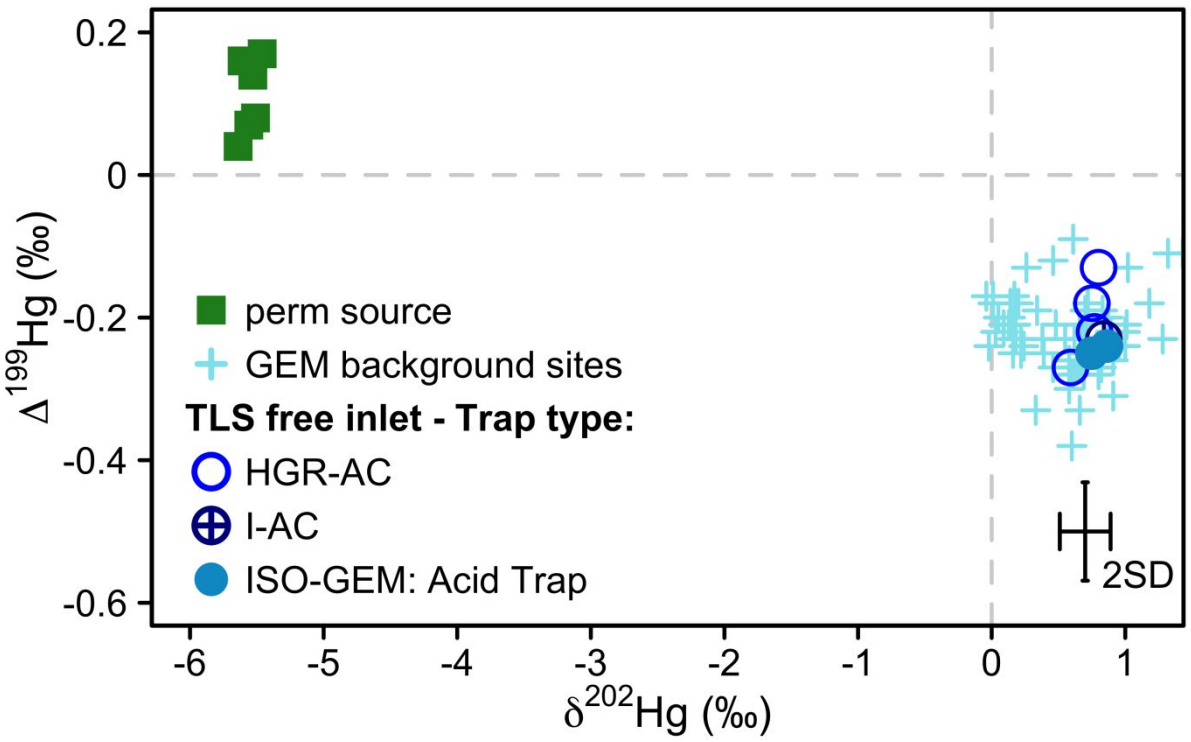

485

486 **Figure 2:** Mass-dependent (δ^{202}Hg) vs. mass-independent (Δ^{199}Hg) Hg isotope signatures
487 of GEM measured by different trap types at the free inlet in Toulouse, France. For
488 comparison, GEM measurements at remote sites[5,6, 7,5, 10] are shown as blue crosses. The
489 isotope signatures of GEM supplied by the internal permeation source of the Tekran®
490 2537X collected with an acid-trap (green squares) serves as internal isotope standard for
491 the ISO-GEM system. The error bars represent the 2 SD of replicate inhouse standard
492 measurements.

493

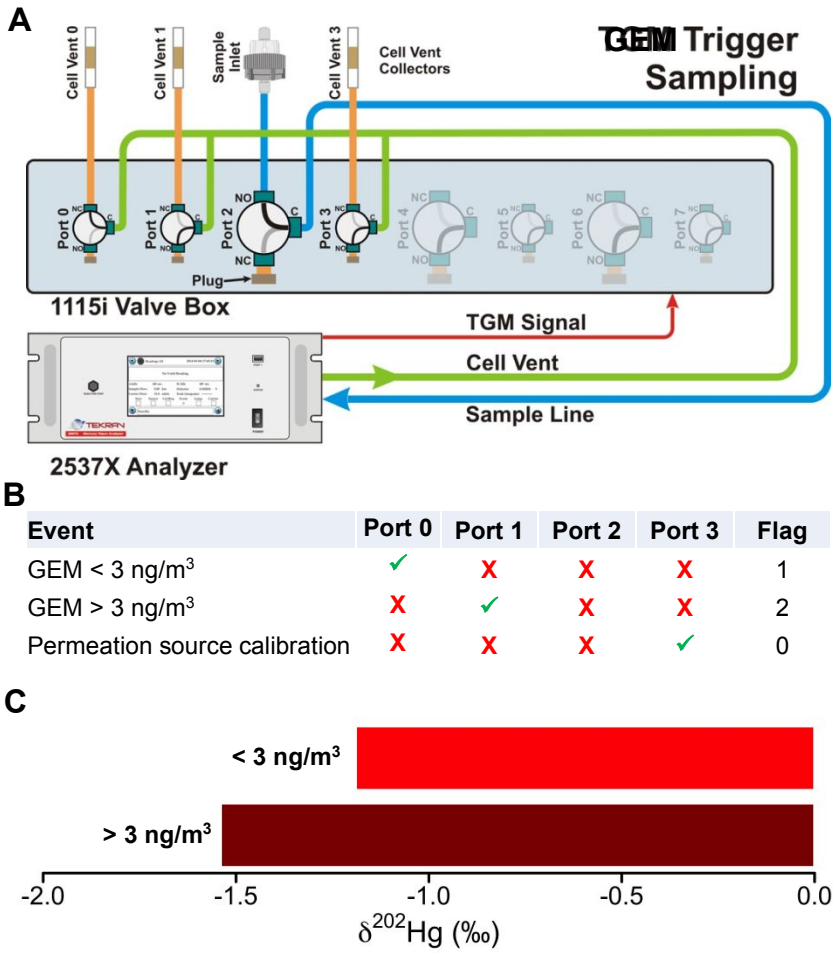

Figure 3: A: ISO-GEM configuration with a GEM threshold event. B: Valve configuration of GEM threshold event. When GEM <3 ng m^{-3}, analyzed GEM at the cell vent is directed to 'port 0' (and trap 0). When GEM > 3 ng m^{-3}, analyzed GEM at the cell vent is directed to 'port 1' (and trap 1). C: δ^{202}Hg of GEM separated by concentration criteria (<3 ng m^{-3}, >3 ng m^{-3}).

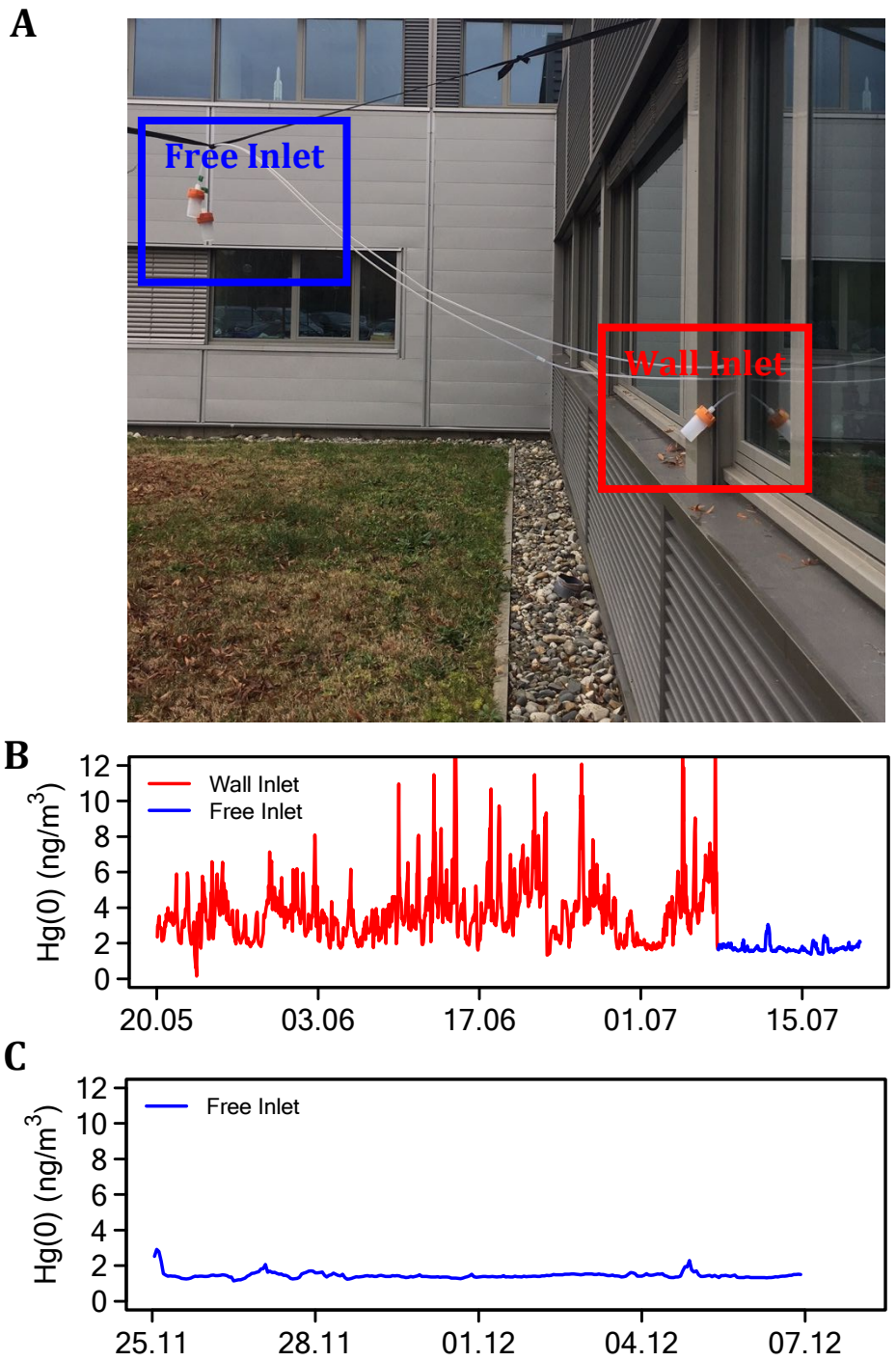

Figure 4: A) Setup of air sampling inlets with the wall inlet (red) and free inlet (blue) **B)** GEM concentration measured from both inlets during summer 2017 **C)** GEM concentration measured during fall 2017.

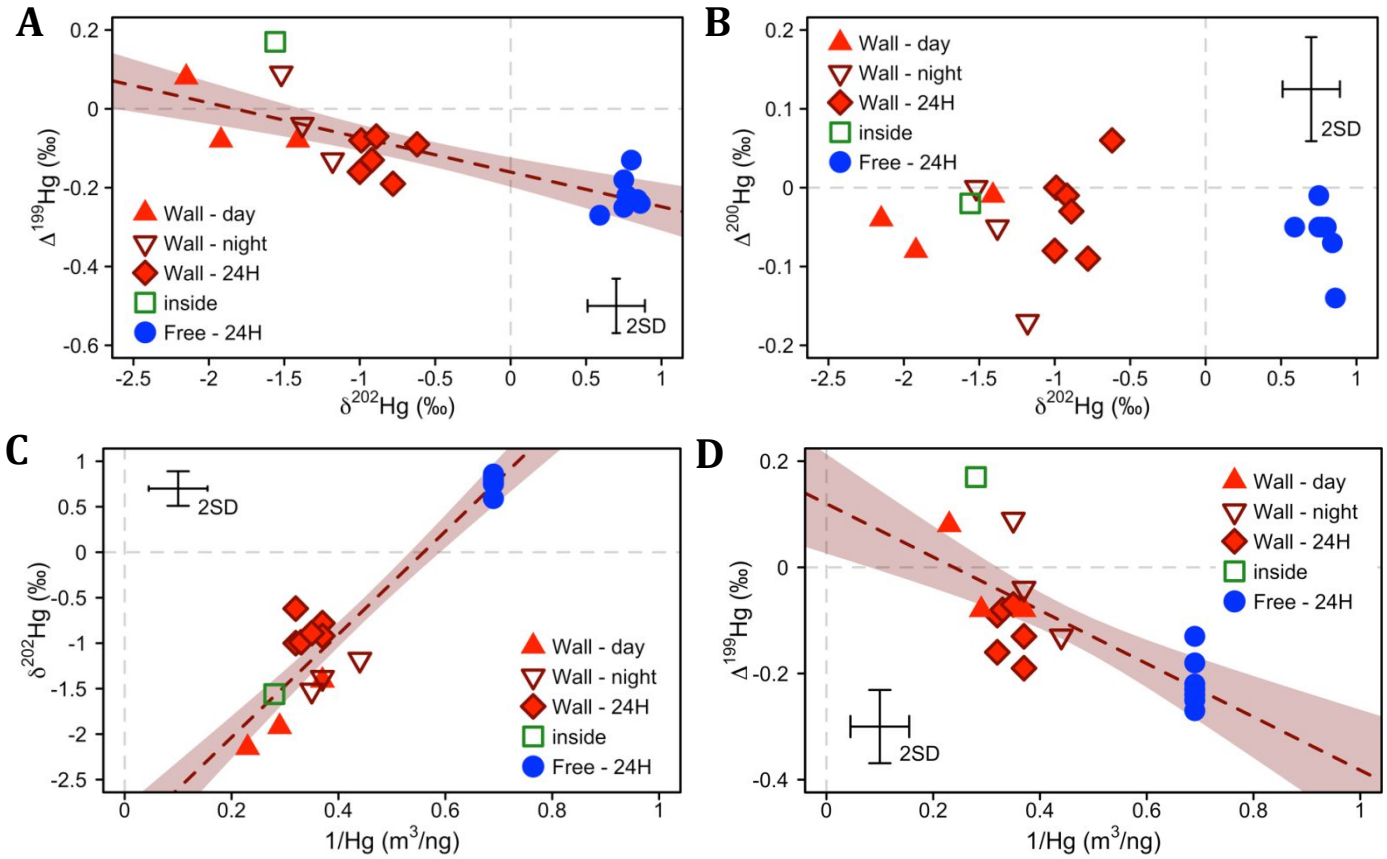

Figure 5: Hg isotope signature of GEM measured at a free inlet (blue circles) and a wall inlet (red triangles and diamonds) outside a laboratory building and inside the laboratory (green squares) in urban Toulouse, France **A)** Δ^{199}Hg vs. δ^{202}Hg, **B)** Δ^{200}Hg vs. δ^{202}Hg, **C)** δ^{202}Hg vs. 1/Hg, and **D)** Δ^{199}Hg vs. 1/Hg.. The dashed lines represent the linear regression and the shaded area represents the 95% confidence interval of the linear regression. The error bars represent the 2 SD of replicate inhouse standard measurements.

TOC ART:

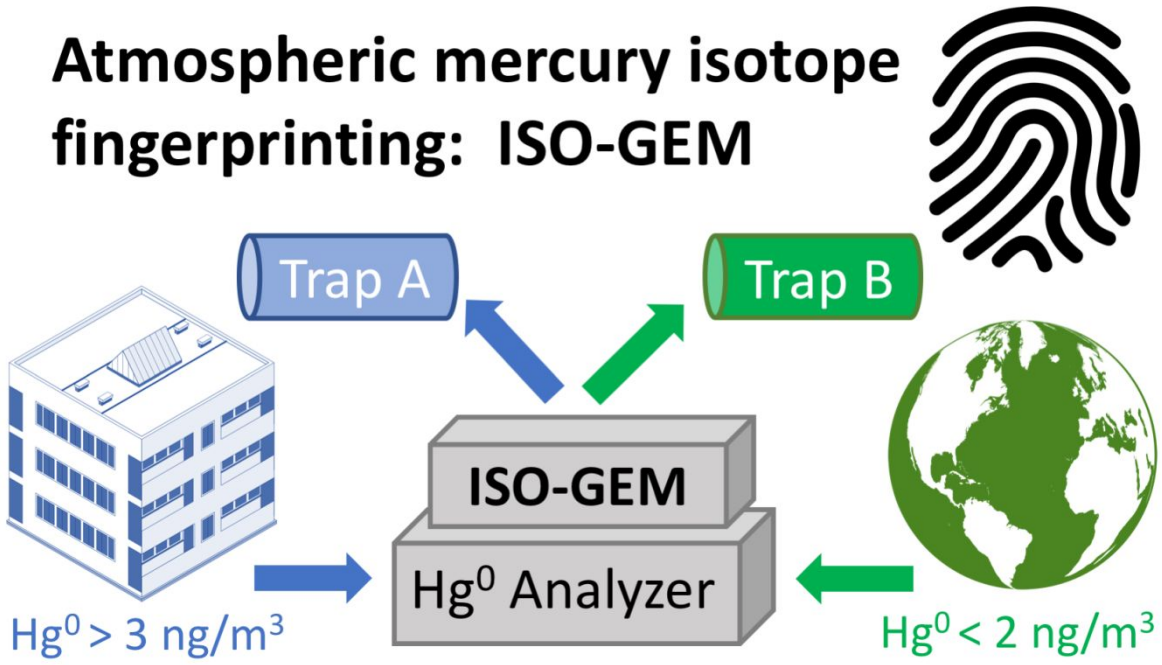
Atmospheric mercury isotope fingerprinting: ISO-GEM
Trap A
Trap B
ISO-GEM
Hg0 Analyzer
Hg0 > 3 ng/m3
Hg0 < 2 ng/m3

588 References
589
590 1. Driscoll, C. T.; Mason, R. P.; Chan, H. M.; Jacob, D. J.; Pirrone, N., Mercury as a
591 global pollutant: sources, pathways, and effects. *Environ. Sci. Technol.* **2013,** *47*,
592 (10), 4967-4983.

593 2. Obrist, D.; Kirk, J. L.; Zhang, L.; Sunderland, E. M.; Jiskra, M.; Selin, N. E., A review
594 of global environmental mercury processes in response to human and natural
595 perturbations: Changes of emissions, climate, and land use. *Ambio* **2018,** *47*, (2),
596 116-140.

597 3. Jiskra, M.; Sonke, J. E.; Obrist, D.; Bieser, J.; Ebinghaus, R.; Myhre, C. L.; Pfaffhuber,
598 K. A.; Wangberg, I.; Kyllonen, K.; Worthy, D.; Martin, L. G.; Labuschagne, C.;
599 Mkololo, T.; Ramonet, M.; Magand, O.; Dommergue, A., A vegetation control on
600 seasonal variations in global atmospheric mercury concentrations. *Nat. Geosci.*
601 **2018,** *11*, (4), 244-+.

602 4. Gratz, L. E.; Keeler, G. J.; Blum, J. D.; Sherman, L. S., Isotopic composition and
603 fractionation of mercury in great lakes precipitation and ambient air. *Environ. Sci.*
604 *Technol.* **2010,** *44*, (20), 7764-7770.

605 5. Demers, J. D.; Sherman, L. S.; Blum, J. D.; Marsik, F. J.; Dvonch, J. T., Coupling
606 atmospheric mercury isotope ratios and meteorology to identify sources of
607 mercury impacting a coastal urban-industrial region near Pensacola, Florida,
608 USA. *Global Biogeochem. Cycles* **2015,** *29*, (10), 1689-1705.

609 6. Fu, X.; Marusczak, N.; Wang, X.; Gheusi, F.; Sonke, J. E., Isotopic Composition of
610 Gaseous Elemental Mercury in the Free Troposphere of the Pic du Midi
611 Observatory, France. *Environ Sci Technol* **2016,** *50*, (11), 5641-50.

612 7. Enrico, M.; Roux, G. L.; Marusczak, N.; Heimburger, L. E.; Claustres, A.; Fu, X.; Sun,
613 R.; Sonke, J. E., Atmospheric mercury transfer to peat bogs dominated by gaseous
614 elemental mercury dry deposition. *Environ Sci Technol* **2016,** *50*, (5), 2405-12.

615 8. Yu, B.; Fu, X.; Yin, R.; Zhang, H.; Wang, X.; Lin, C. J.; Wu, C.; Zhang, Y.; He, N.; Fu, P.;
616 Wang, Z.; Shang, L.; Sommar, J.; Sonke, J. E.; Maurice, L.; Guinot, B.; Feng, X.,
617 Isotopic Composition of Atmospheric Mercury in China: New Evidence for
618 Sources and Transformation Processes in Air and in Vegetation. *Environ Sci*
619 *Technol* **2016,** *50*, (17), 9262-9.

9. Yamakawa, A.; Moriya, K.; Yoshinaga, J., Determination of isotopic composition of atmospheric mercury in urban-industrial and coastal regions of Chiba, Japan, using cold vapor multicollector inductively coupled plasma mass spectrometry. *Chemical Geology* **2017,** *448*, 84-92.

10. Obrist, D.; Agnan, Y.; Jiskra, M.; Olson, C. L.; Colegrove, D. P.; Hueber, J.; Moore, C. W.; Sonke, J. E.; Helmig, D., Tundra uptake of atmospheric elemental mercury drives Arctic mercury pollution. *Nature* **2017,** *547*, (7662), 201-204.

11. Demers, J. D.; Blum, J. D.; Zak, D. R., Mercury isotopes in a forested ecosystem: Implications for air-surface exchange dynamics and the global mercury cycle. *Global Biogeochem. Cycles* **2013,** *27*, (1), 222-238.

12. Fu, X.; Yang, X.; Tan, Q.; Ming, L.; Lin, T.; Lin, C.-J.; Li, X.; Feng, X., Isotopic Composition of Gaseous Elemental Mercury in the Marine Boundary Layer of East China Sea. *Journal of Geophysical Research: Atmospheres* **2018,** *123*, (14), 7656-7669.

13. Biswas, A.; Blum, J. D.; Bergquist, B. A.; Keeler, G. J.; Xie, Z. Q., Natural Mercury Isotope Variation in Coal Deposits and Organic Soils. *Environ. Sci. Technol.* **2008,** *42*, (22), 8303-8309.

14. Sun, R.; Sonke, J. E.; Heimburger, L. E.; Belkin, H. E.; Liu, G.; Shome, D.; Cukrowska, E.; Liousse, C.; Pokrovsky, O. S.; Streets, D. G., Mercury stable isotope signatures of world coal deposits and historical coal combustion emissions. *Environ. Sci. Technol.* **2014,** *48*, (13), 7660-7668.

15. Yin, R.; Feng, X.; Chen, J., Mercury Stable Isotopic Compositions in Coals from Major Coal Producing Fields in China and Their Geochemical and Environmental Implications. *Environmental Science & Technology* **2014,** *48*, (10), 5565-5574.

16. Zheng, W.; Obrist, D.; Weis, D.; Bergquist, B. A., Mercury isotope compositions across North American forests. *Global Biogeochem. Cycles* **2016,** *30*, (10), 1475-1492.

17. Jiskra, M.; Wiederhold, J. G.; Skyllberg, U.; Kronberg, R. M.; Hajdas, I.; Kretzschmar, R., Mercury deposition and re-emission pathways in boreal forest soils investigated with Hg isotope signatures. *Environ Sci Technol* **2015,** *49*, (12), 7188-96.

18. Sherman, L. S.; Blum, J. D.; Johnson, K. P.; Keeler, G. J.; Barres, J. A.; Douglas, T. A., Mass-independent fractionation of mercury isotopes in Arctic snow driven by sunlight. *Nat. Geosci.* **2010,** *3*, (3), 173-177.

19. Fu, X.; Heimburger, L.-E.; Sonke, J. E., Collection of atmospheric gaseous mercury for stable isotope analysis using iodine- and chlorine-impregnated activated carbon traps. *J. Anal. At. Spectrom.* **2014,** *29*, (5), 841-852.

20. Fu, X.; Zhu, W.; Zhang, H.; Sommar, J.; Yu, B.; Yang, X.; Wang, X.; Lin, C. J.; Feng, X., Depletion of atmospheric gaseous elemental mercury by plant uptake at Mt. Changbai, Northeast China. *Atmos. Chem. Phys.* **2016,** *16*, (20), 12861-12873.

21. Sprovieri, F.; Pirrone, N.; Bencardino, M.; D'Amore, F.; Carbone, F.; Cinnirella, S.; Mannarino, V.; Landis, M.; Ebinghaus, R.; Weigelt, A.; Brunke, E. G.; Labuschagne, C.; Martin, L.; Munthe, J.; Wängberg, I.; Artaxo, P.; Morais, F.; Barbosa, H. D. M. J.; Brito, J.; Cairns, W.; Barbante, C.; Diéguez, M. D. C.; Garcia, P. E.; Dommergue, A.; Angot, H.; Magand, O.; Skov, H.; Horvat, M.; Kotnik, J.; Read, K. A.; Neves, L. M.; Gawlik, B. M.; Sena, F.; Mashyanov, N.; Obolkin, V.; Wip, D.; Feng, X. B.; Zhang, H.; Fu, X.; Ramachandran, R.; Cossa, D.; Knoery, J.; Marusczak, N.; Nerentorp, M.; Norstrom, C., Atmospheric mercury concentrations observed at ground-based monitoring sites globally distributed in the framework of the GMOS network. *Atmos. Chem. Phys.* **2016,** *16*, (18), 11915-11935.

22. McLagan, D. S.; Mitchell, C. P. J.; Huang, H.; Lei, Y. D.; Cole, A. S.; Steffen, A.; Hung, H.; Wania, F., A High-Precision Passive Air Sampler for Gaseous Mercury. *Environmental Science & Technology Letters* **2016,** *3*, (1), 24-29.

23. McLagan, D. S.; Mitchell, C. P. J.; Steffen, A.; Hung, H.; Shin, C.; Stupple, G. W.; Olson, M. L.; Luke, W. T.; Kelley, P.; Howard, D.; Edwards, G. C.; Nelson, P. F.; Xiao, H.; Sheu, G. R.; Dreyer, A.; Huang, H.; Abdul Hussain, B.; Lei, Y. D.; Tavshunsky, I.; Wania, F., Global evaluation and calibration of a passive air sampler for gaseous mercury. *Atmos. Chem. Phys. Discuss.* **2018,** *2018*, 1-32.

24. Sun, R. Y.; Enrico, M.; Heimburger, L. E.; Scott, C.; Sonke, J. E., A double-stage tube furnace-acid-trapping protocol for the pre-concentration of mercury from solid samples for isotopic analysis. *Anal. Bioanal. Chem.* **2013,** *405*, (21), 6771-6781.

25. McLagan, D. S.; Huang, H.; Lei, Y. D.; Wania, F.; Mitchell, C. P. J., Application of sodium carbonate prevents sulphur poisoning of catalysts in automated total

mercury analysis. *Spectrochimica Acta Part B: Atomic Spectroscopy* **2017,** *133*, 60-62.

26. *Method 1631, Revision E: Mercury in Water by Oxidation, Purge and Trap, and Cold Vapor Atomic Fluorescence Spectrometry*; United States Environment Protection Agency: https://www.epa.gov/sites/production/files/2015-08/documents/method_1631e_2002.pdf , Washington, DC, 2002.

27. Smith, R. S.; Wiederhold, J. G.; Jew, A. D.; Brown, G. E.; Bourdon, B.; Kretzschmar, R., Stable Hg Isotope Signatures in Creek Sediments Impacted by a Former Hg Mine. *Environmental Science & Technology* **2015,** *49*, (2), 767-776.

28. Stamenkovic, J.; Lyman, S.; Gustin, M. S., Seasonal and diel variation of atmospheric mercury concentrations in the Reno (Nevada, USA) airshed. *Atmospheric Environment* **2007,** *41*, (31), 6662-6672.

29. Lan, X.; Talbot, R.; Laine, P.; Lefer, B.; Flynn, J.; Torres, A., Seasonal and Diurnal Variations of Total Gaseous Mercury in Urban Houston, TX, USA. *Atmosphere* **2014,** *5*, (2), 399-419.

30. Carpi, A.; Chen, Y.-f., Gaseous Elemental Mercury as an Indoor Air Pollutant. *Environmental Science & Technology* **2001,** *35*, (21), 4170-4173.

31. Horowitz, H. M.; Jacob, D. J.; Amos, H. M.; Streets, D. G.; Sunderland, E. M., Historical mercury releases from commercial products: global environmental implications. *Environ. Sci. Technol.* **2014,** *48*, (17), 10242-50.

32. Carpi, A.; Chen, Y.-f., Gaseous Elemental Mercury Fluxes in New York City. *Water, Air, and Soil Pollution* **2002,** *140*, (1), 371-379.

33. Xu, X. H.; Akhtar, U.; Clark, K.; Wang, X. B., Temporal Variability of Atmospheric Total Gaseous Mercury in Windsor, ON, Canada. *Atmosphere* **2014,** *5*, (3), 536-556.

34. Cairns, E.; Tharumakulasingam, K.; Athar, M.; Yousaf, M.; Cheng, I.; Huang, Y.; Lu, J.; Yap, D., Source, concentration, and distribution of elemental mercury in the atmosphere in Toronto, Canada. *Environ. Pollut.* **2011,** *159*, (8), 2003-2008.

712 35. Fu, X.; Feng, X.; Qiu, G.; Shang, L.; Zhang, H., Speciated atmospheric mercury and
713 its potential source in Guiyang, China. *Atmospheric Environment* **2011,** *45*, (25),
714 4205-4212.

715 36. Chen, J.; Hintelmann, H.; Feng, X.; Dimock, B., Unusual fractionation of both odd
716 and even mercury isotopes in precipitation from Peterborough, ON, Canada.
717 *Geochim. Cosmochim. Acta* **2012,** *90*, (0), 33-46.

718 37. Sherman, L. S.; Blum, J. D.; Keeler, G. J.; Demers, J. D.; Dvonch, J. T., Investigation of
719 local mercury deposition from a coal-fired power plant using mercury isotopes.
720 *Environ. Sci. Technol.* **2012,** *46*, (1), 382-90.

721 38. Chesworth, W., Use of aluminum-amalgam in mineral synthesis at low
722 temperatures and 1 atmosphere total pressure. *Clays and Clay Minerals* **1971,** *19*,
723 (5), 337-339.

724 39. Estrade, N.; Carignan, J.; Sonke, J. E.; Donard, O. F. X., Mercury isotope
725 fractionation during liquid-vapor evaporation experiments. *Geochim. Cosmochim.*
726 *Acta* **2009,** *73*, (10), 2693-2711.

727 40. Ghosh, S.; Schauble, E. A.; Lacrampe Couloume, G.; Blum, J. D.; Bergquist, B. A.,
728 Estimation of nuclear volume dependent fractionation of mercury isotopes in
729 equilibrium liquid–vapor evaporation experiments. *Chem. Geol.* **2013,** *336*, 5-12.

730 41. NADP *NADP Site Selection and Installation Manual*; http://nadp.isws.illinois.edu,
731 11.2014, 2014.

732 42. GMOS *GMOS Standard Operational Procedure: Methods for the determination of*
733 *TGM and GEM*; http://www.gmos.eu/index.php/gmos-standard-operating-
734 procedures-sops, 7.4.2011, 2011.

735

736

737

738